**BioRxiv**

10 February 2023

# Modulation of the E-cadherin in human cells infected *in vitro* with *Coxiella burnetii*

Running title: E-cadherin pathway modulation during *Coxiella burnetii* infection

Ikram OMAR OSMAN[1,2], Soraya MEZOUAR[1,2], Djamal BELHAOUARI-BRAHIM[1,2], Jean-Louis MEGE[1,2], Christian Albert DEVAUX[1,2,3*].

[1]Aix-Marseille Univ, IRD, APHM, MEPHI, Marseille, France

[2]IHU-Méditerranée Infection, Marseille, France

[3]CNRS, Marseille, France

**[*]Corresponding author:**

Christian Devaux, PhD

Email: christian.devaux@mediterranee-infection.com

**Abstract :**

High concentration of soluble E-cadherin (E-cad) was previously found in sera from Q fever patients. Here, BeWo cells which express a high concentration of E-cad were used as an *in vitro* model to investigate the expression and function of E-cad in response to infection by *Coxiella burnetii*, the etiological agent of Q fever. Infection of BeWo cells with *C. burnetii* leads to a decrease in the number of BeWo cells expressing E-cad at their membrane. A shedding of soluble E-cad was associated with the post-infection decrease of membrane-bound E-cad. The modulation of E-cad expression requires bacterial viability and was not found with heat-inactivated *C. burnetii*. Moreover, the intracytoplasmic cell concentration of β-catenin (β-cat), a ligand of E-cad, was reduced after bacterial infection, suggesting that the bacterium induces modulation of the E-cad/β-cat signaling pathway and *CDH1* and *CTNNB1* genes transcription. Finally, several genes operating the canonical Wnt-Frizzled/β-cat pathway were overexpressed in cells infected with *C. burnetii*. This was particularly evident with the highly virulent strain of *C. burnetii,* Guiana. Our data demonstrate that infection of BeWo cells by live *C. burnetii* modulates the E-cad/β-cat signaling pathway.

Key Words: *Coxiella burnetii*; E-cadherin; Soluble E-cadherin; β-catenin

51 **Introduction**

52 *Coxiella burnetii*, a known intracellular bacterium causing Query (Q) fever in humans, is most
53 often transmitted to humans through products derived from infected animals[1], and primarily
54 targets the lungs. The bacterium infects a large spectrum of susceptible cells, including myeloid
55 cells[2,3], trophoblasts[4] and adipocytes[5]. Human primary infection remains asymptomatic in
56 most people (around 60% of cases)[6]. In the other cases, symptoms develop within 2-6 weeks
57 after *C. burnetii* exposure and mainly consist of hepatitis, endocarditis, pneumonia, vascular
58 infection and lymphadenitis[7,8]. Although these symptoms usually resolve in a few weeks, in rare
59 cases (less than 5%), the infection become persistent and progresses to chronic endocarditis[9].
60 Factors that may determine the severity of the disease remain mostly unknown[10–13], but
61 considerable genomic heterogeneity was reported among *C. burnetii* strains[14–18], and gene
62 deletion was associated with a higher strain virulence[19]. A role for the bacterial
63 lipopolysaccharide (LPS) was also highlighted, since several *in vitro* passages of the virulent Nine
64 Mile strain of *C. burnetii* generate an avirulent strain characterized by a truncated LPS with the
65 absence of the terminal sugar-containing O-polysaccharide chain[19,20].

66 In the past decade, a diagnosis of Q fever with persistent focal infection was reported as an
67 increased risk factor for B-cell lymphoma [21–23]. Overproduction of interleukin (IL)-10, a B-cell
68 growth factor[24], is critical for sustaining *C. burnetii* replication[25], and might possibly favor
69 lymphoma occurrence [22]. In peripheral blood mononuclear cells (PBMCs) of Q fever patients it
70 was possible to characterize a transcriptional signature (overexpression of genes involved in the
71 anti-apoptotic process or repression of pro-apoptotic pathways), that could be, in very rare cases,
72 associated with the development of non-Hodgkin lymphoma (NHL)[26]. We also speculated that
73 if *C. burnetii* infection could sometimes promote the development of NHL, the early steps towards

74 NHL progression might be the decrease of E-cadherin (E-cad) surface expression on the $CD20^+$ B-
75 cells subpopulation of PBMCs (E-cad positive B-cells represents less than 1% of the circulating B
76 lymphocytes) from *C. burnetii*-infected patients [27]. However, until now the molecular
77 mechanisms that could account for the progression of the disease to lymphoma have remained
78 elusive. Moreover, these results are controversial, and other studies of Q fever patients have not
79 confirmed the link between Q fever and NHL[28]. A recent large analysis of the Dutch population
80 incorporating the 2007-2010 Q fever outbreak (266 million people including 61424 diagnosed with
81 NHL and 4310 persons diagnosed with acute Q fever), concluded to the lack of increased risk of
82 NHL after Q fever[29].
83 We previously found that sE-cad is present in higher concentrations in sera of Q fever patients than
84 healthy controls[27], and postulated that E-cad cleavage may be a step towards *C. burnetii*-invasion
85 of the host during Q fever. Increasing evidence can be found in the literature indicating that
86 cadherins may play a major role during the development of infectious diseases[30]. Among
87 cadherins, the E-cadherin (E-cad), a 120 kDa adhesion cell-surface protein, is known for its role in
88 cell-to-cell tight junctions ensuring integrity of epithelial barriers. E-cad also behaves as a signaling
89 molecule through its intra-cytoplasmic tail that binds second messengers, thereby having roles in
90 cell activation, cell division, and cell differentiation and/or invasion[31,32]. Besides its role in
91 inter-cellular adhesion, E-cad behaves as a tumor suppressor[33–35] and plays a major role in
92 cancer invasion/metastasis[36–38]. Cell reprogramming can be achieved by the release of sE-cad
93 generated from the cleavage of the extracellular domain of E-cad[39]. E-cad is known to be a target
94 for several bacterial sheddases, leading to the release of sE-cad[39,40].
95 Here we developed an *in vitro* cellular model with BeWo cells which express a high concentration
96 of E-cad at their surface[41] and are susceptible to *C. burnetii* infection[4] to study the effect of *C.*
97 *burnetii* infection on the expression of E-cad and evidenced that *C. burnetii* infection modulates

expression of the E-cad/β-catenin signaling pathway by acting on *CDH1* and *CTNNB1* gene transcription, on cell-surface expression of E-cad, the release of sE-cad and the cytosolic pool of β-catenin.

119 ## Materials and Methods

120 ***Coxiella burnetii***

121 *Coxiella burnetii* (Nine Mile strain RSA496, Guiana Strain Cb175) was grown as described[42].
122 L929 cells line were used for *in vitro* culture using a Minimum Eagle medium (MEM, Invitrogen,
123 USA) supplemented with 4% fetal bovine serum (FBS, Invitrogen, USA) and 1% 2mM L-
124 glutamine (Invitrogen, USA) and then incubated at 35°C in a 5% $CO_2$ atmosphere. After three
125 passages infected cells were sonicated, and the cell-free supernatants were centrifuged to harvest
126 the bacteria, which were then washed and stored at -80°C until use. Gimenez staining and qPCR
127 (using the *com-1* gene) were used to determine the concentration of bacteria in the sample.

128

129 ***In vitro* cell culture model**

130 Blood samples (leucopacks) used in our study come from the French Blood Establishment
131 (Etablissement français du sang, EFS), which carries out donor inclusions, informed consent and
132 sample collection. Through a convention established between our laboratory and the EFS
133 (No.7828), buffy coats were obtained from healthy blood donors. Peripheral blood mononuclear
134 cells (PBMCs) were isolated after centrifugation on Ficoll cushions (MSL, Eurobio, France).
135 Monocytes (5-15% of the total number of PBMCs) were obtained from PBMCs using magnetic
136 beads coated with monoclonal Abs directed against CD14, according to the manufacturer's
137 instructions (Miltenyi Biotech, France). Monocytes-derived-macrophages (MDM) were obtained
138 following the incubation of monocytes with 10% heat-inactivated human AB serum (MP
139 Biomedicals, LLC, France) during a 3-day culture followed by 4 days of incubation with 10% FBS
140 (Invitrogen, USA) as previously described[43]. Monocyte-derived- dendritic cells (moDC) were
141 obtained by incubation of monocytes with 1 ng/mL of granulocytes-macrophages colony-

142 stimulating factor (GM-CSF, R&D Systems, France) and Interleukin-4 (R&D Systems, USA) for
143 7 days as previously described[44]. Mast cells were obtained from PBMCs as previously
144 described[45]. All cells were cultured in Roswell Park memorial institute (RPMI) 1640 medium
145 (Gibco, Thermo Fisher, USA) supplemented with 10% FBS.
146 The human trophoblastic BeWo cell line was purchased from the American type culture collection
147 (ATCC, CCL-98, Bethesda, USA) and cultured in a Dulbecco's Modified Eagle Medium F-12
148 Nutrient Mixture (DMEM F-12, Invitrogen, USA) containing 10% FBS. The HeLa cell line (ATCC
149 CCL-2), a human epithelial cell line derived from a cervical cancer, was cultured in DMEM
150 supplemented with 10% FBS and 1% L-glutamine (Invitrogen, USA). MRC-5 (ATCC CCL-171),
151 a human embryonic fibroblast cell line obtained from an aborted fetus, was cultured in MEM
152 supplemented with 4% FBS and 1% L-glutamine. THP-1 (ATCC TIB-202), a human monocytic
153 cell line derived from an acute monocytic leukemia patient, was maintained in RPMI 1640 medium
154 supplemented with 10% FBS and 1% penicillin/streptomycin (Gibco) at 37°C and 5% $CO_2$.
155
156 **Microarray and data analysis**
157 The microarray was performed as previously described[26] with data submitted to NCBI's Gene
158 Expression Omnibus (GEO series accession number GSE112086). Briefly, RNAs were extracted
159 using an RNeasy Mini Kit (QIAGEN SA, France) with a DNase I step, then labeled using Cyanin-
160 3 CTP (Agilent Technologies) and hybridized on chips containing 45000 probes (4x44K Whole
161 Human Genome). After hybridization, slides were washed and scanned with a pixel size of 5 µm
162 using the DNA Microarray scanner G2505C. The raw data were extracted (Extraction Software
163 10.5.1) and processed using GeneSpring GX 14.9 software (Agilent Technologies). A selection
164 filter of both statistical value $p<0.01$ (t-Student test) and an absolute value of fold change (FC)

165 greater than 1.5 was used to identify differentially expressed genes. Modulated genes were
166 analyzed using ClustVis software.
167
168 **Quantitative-Reverse Transcription Polymerase Chain Reaction (qRT-PCR)**
169 BeWo cells ($2x10^5$ cells/well) were cultured in flat-bottom 24-well plates for 12 h and were then
170 infected with the live virulent *C. burnetii* Nine Mile (NMI) and Guiana (GuiI) strains or were
171 exposed to heat-inactivated virulent *C. burnetii* NMI strains at a 100:1 bacterium-to-cell ratio, or
172 stimulated with 100 ng/mL of lipopolysaccharide (LPS) from *E. Coli* (O55:B5; Sigma-Aldrich,
173 USA) for 48 h at 37°C in a 5% $CO_2$ atmosphere. RNAs were extracted as described above. The
174 first-strand cDNA was obtained using oligo(dT) primers and Moloney murine leukemia virus-
175 reverse transcriptase (MMLV-RT kit; Life Technologies, USA), using 100 ng of purified RNA.
176 The qPCR experiments were performed using specific oligonucleotide primers and hot-start
177 polymerase (SYBR Green Fast Master Mix; Roche Diagnostics, Germany). The amplification
178 cycles were performed using a C1000 Touch Thermal cycler (Biorad, USA). Specific primers used
179 in this study are listed in **Table 1** and the results were normalized using the housekeeping gene β-
180 actin (*ACTB*) (Fwd: 5' CAT GCC ATC CTG CGT CTG GA 3'; Rev: 5' CCG TGG CCA TCT CTT
181 GCT CG 3') and expressed as the relative expression ($2^{-\Delta CT}$) where $\Delta Ct = Ct_{Target} - Ct_{Actin}$, and as
182 the fold change ($2^{-\Delta\Delta CT}$), where $\Delta\Delta Ct = \Delta Ct_{stimulated} - \Delta Ct_{unstimulated}$ as previously described[46]. Ct
183 values were defined as the number of cycles for which fluorescence signals were detected.
184
185
186
187
188

189 **E-cadherin protein quantification**

190 BeWo cells ($5x10^5$ cells/well) were cultured in flat-bottom 12-well plates for 12 h and were then
191 infected with live *C. burnetii* NMI strains or exposed to heat-inactivated *C. burnetii* strains at a
192 50:1 bacterium-to-cell ratio or stimulated with 100 ng/mL of LPS for 4, 24 and 48 h at 37°C in a
193 5% $CO_2$ atmosphere.

194 For each kinetics, the culture supernatants were collected, centrifuged at 1000 g for 10 min and
195 stored at -20°C until use. The quantity of sE-cad in the supernatants was determined using a specific
196 immunoassay (DCADEO, R&D Systems, USA) according to the manufacturer's instructions. The
197 minimal detectable concentration of human sE-cad was 0.313 ng/mL.

198 Protein quantification was evaluated using a western blot assay. Cells were washed with ice cold
199 phosphate buffered saline (PBS 1X) and lysed using 1X RIPA buffer (100 mM Tris-HCl pH 7.5,
200 750 mM NaCl, 5 mM EDTA, 5% IGEPAL, 0.5% sodium dodecyl sulfate (SDS), and 2.5% Na
201 deoxycholate) supplemented with both a protease and phosphatase cocktail inhibitor (Roche,
202 Germany). Ten µg of protein were loaded onto 10% SDS polyacrylamide gels. After transfer into
203 a nitrocellulose membrane, the blots were incubated overnight at 4°C with a saturation solution
204 (5% fat free milk (FFM)-1X PBS - 0.3% Tween 20). Blots were then incubated with mouse anti-
205 human E-cad ectodomain mAb (1:5000) (HECD-131700, Invitrogen, USA) for 2 h, followed by
206 an incubation with mouse anti-human E-cad cytoplasmic domain mAb (4A2C7, Life
207 Technologies). In some experiments, β-catenin was detected using an anti-human β-catenin
208 antibody (1:1000) (Agilent Dako, USA). After three washes in 1X PBS – 0.3% Tween 20, the blots
209 were incubated with horseradish peroxidase-conjugated sheep anti-mouse IgG (1:10000) for 2 h at
210 room temperature. β-actin expression was measured using an anti-human β-actin horseradish
211 peroxidase-conjugated mAb (1:25000, Life Technologies, USA) as the loading control. The
212 proteins were revealed using an ECL western blotting substrate (Promega, USA) and images were

213 digitized using a Fusion FX (Vilber Lourmat, France). The density of the bands was measured
214 using Image J v 1.8.0.
215
216 **Confocal immunofluorescence assay**
217 BeWo cells were cultured on sterile coverslips in 24-well plates at an initial concentration of $2\times10^5$
218 cells/well and were then infected with live virulent *C. burnetii* NMI strains or exposed to heat-
219 inactivated virulent *C. burnetii* NMI strain at a 50:1 bacterium-to-cell ratio or stimulated with 100
220 ng/mL LPS for 24 h at 37°C in a 5% $CO_2$ atmosphere. After fixation with 4% paraformaldehyde,
221 cells were permeabilized with 0.1% Triton X-100 for 3 min and saturated with 3% BSA – 0.1%
222 Tween 20 - PBS for 30 min at room temperature. Fixed cells were first incubated with a mouse
223 anti-E-cad cytoplasmic domain mAb (1:1000) (4A2C7, Life Technologies, USA) for 1 h at room
224 temperature and then with 1:500 rabbit polyclonal anti-*C. burnetii* antiserum. After washing, cells
225 were incubated for 30 min at room temperature with a mix (1:1000) of goat anti-rabbit IgG
226 secondary antibody (Alexa Fluor 647, Life Technologies, USA) and goat anti-mouse IgG
227 secondary antibody (Alexa Fluor-555, Life Technologies, USA). 4',6'-diamino-2-fenil-indol
228 (1:25000) (DAPI, Life Technologies, USA) and Phalloidin (1:500) (Alexa-488, OZYME, France)
229 were used for staining the nucleus and the filamentous actin, respectively. Labelled cells were
230 analyzed using laser scanning confocal microscopy and pictures were acquired using a confocal
231 microscope (Zeiss LSM 800) with a 63X/1.4 oil objective, an electronic magnification of 0.7 and
232 a resolution of 1014_1014 pixels.
233
234 **Flow cytometry assay**
235 BeWo cells ($1\times10^6$ cells/well) were cultured in flat-bottom 6-well plates and were then infected
236 with a live virulent *C. burnetii* NMI strain at a 50:1 bacterium-to-cell ratio or stimulated with 100

237 ng/mL LPS for 24, 48 and 72 h at 37°C in a 5% $CO_2$ atmosphere. Cells were incubated with 2 mM
238 EDTA in PBS for 15 min at 4°C to release the adherent cells from the culture plate. After
239 centrifugation at 500 g for 5 min, the pellet was suspended in a FACS buffer (2 mM EDTA, 10%
240 FBS in PBS) and then incubated for 30 min with a mouse anti-human E-cad ectodomain antibody
241 (HECD-131700, 1:1000). After two washes, cells were incubated with a goat anti-mouse IgG Alexa
242 Fluor-555 secondary antibody. Fluorescence intensity was measured using a Canto II
243 cytofluorometer (Becton Dickinson/Biosciences, France) and the results were analyzed using
244 FlowJo V10.7.2 software (Becton Dickinson, USA).
245
246 **Electron microscopy analysis**
247 BeWo cells ($1\times10^6$ cells/well) were cultured in flat-bottom 6-well plates and were then infected
248 with live virulent *C. burnetii* NMI and GuiI strains at a 100:1 bacterium-to-cell ratio at 37°C in a
249 5% $CO_2$ atmosphere. After 24 h of infection, the cells were fixed with 2.5% glutaraldehyde in 0.1
250 M cacodylate buffer for five hours at 4°C. Resin embedding was microwave-assisted with a
251 Biowave Pro+ (Pelco, Fresno, CA, USA). After washing twice with a mixture of 0.2-M
252 saccharose/0.1-M sodium cacodylate and once with distilled water, samples were progressively
253 dehydrated by successive baths in 50%, 70% and 96% ethanol. Substitution with LR–White resin
254 (medium grade; Polysciences, Warrington, PA, USA) was achieved by incubations with 25% to
255 100% LR–White resin and samples were placed in a polymerization chamber for 72 h at 60°C. All
256 solutions used above were 0.2-µm filtered. After curing, the resin blocks were manually trimmed
257 with a razor blade and dish bottoms were detached from cell monolayers by cold shock via
258 immersion in liquid nitrogen for 20 seconds. Resin blocks were placed in a UC7 ultramicrotome
259 (Leica), trimmed to pyramids, and ultrathin 100 nm sections were cut and placed on HR25 300
260 Mesh Copper/Rhodium grids (TAAB, Aldermaston, England). Sections were contrasted with

261 uranyl acetate and lead citrate. Grids were attached with double sided tape to a glass slide and
262 platinum-coated at 10 mA for 20 seconds with a MC1000 sputter coater (Hitachi High-
263 Technologies, Japan). Electron micrographs were obtained on a SU5000 SEM (Hitachi High-
264 Technologies, Japan) operated in high-vacuum at 10 kV accelerating voltage and observation mode
265 (spot size 30) with BSE detector.
266
267 **Statistical analysis**
268 The statistical analyses of the data were performed using GraphPad-Prism software (version 6.0).
269 The results are presented as the ± standard error of the mean (SEM). The Mann-Whitney U test
270 was used for flow cytometry, the two-way ANOVA test for E-cadherin quantification and
271 transcriptional analysis, and a nonparametric Kruskal-Wallis with Dunn's multiple comparison test
272 for group comparison. A p value <0.05 was considered statistically significant.
273
274 ## Results
275 **Selection of the BeWo cell line as an appropriate cellular model to study E-cad expression in**
276 **cells infected with *C. burnetii***
277 It was previously reported that many cell types, including myeloid cells[47,48], trophoblasts[4,49],
278 lung cells[50,51], and adipocytes[5] are susceptible to *C. burnetii* infection. To conduct our study,
279 it was first necessary to select a cellular model with high expression of E-cad. To this end, we
280 evaluated E-cad expression in different cell lines, including HeLa (human cervical cancer cell line),
281 THP-1 (human monocytic cell line), MRC-5 (human fetal lung fibroblasts), BeWo (human placenta
282 choriocarcinoma cell line), and primary monocytes from healthy donors. As shown in **Figure 1A**,
283 using a western blot assay, BeWo cells were found to express the highest concentration of E-cad

284 and HeLa cells ranked second. Additionally, we also confirmed the highest membrane expression
285 of E-cad on BeWo cells by confocal microscopy (**Figure 1B**). This finding was consistent with the
286 reports from the literature on the common use of BeWo cells as a model to study E-cad
287 expression[52,53]. Moreover, scanning electron microscopy of *C. burnetii*-infected BeWo cells
288 (**Figure 1C** and **Figure S1**) showed the presence of several vacuoles, either empty or containing
289 electron-dense circular structures, with diameters ranging from 250 nm to 700 nm dispersed in the
290 cell cytoplasm, corresponding to the morphology and size of *C. burnetii* as previously
291 described[54]. Therefore, the BeWo cell line was chosen for further investigation because it has
292 both sensitivity to *C. burnetii* infection and high expression of E-cad.
293
294 ***C. burnetii* infection modulates cell surface expression of E-cad**
295 The level of E-cad protein expression at the cell surface of BeWo cells infected or not by *C. burnetii*
296 NMI was evaluated by flow cytometry, targeting the ectodomain portion of E-cad. Twenty-four
297 hours post-*C. burnetii* infection, the percentage of BeWo cells expressing membrane-bound E-cad
298 decreased significantly compared to LPS stimulated- and unstimulated- cells ($p<0.05$ and $p<0.01$,
299 respectively) used as controls (**Figure 2A and 2B**). Also, we found a significant decrease in the
300 mean intensity fluorescence signal of the E-cad in BeWo cells infected with *C. burnetii* compared
301 to LPS-stimulated and unstimulated cells ($p<0.05$ and $p<0.01$, respectively) (**Figure 2C**). Then,
302 we studied whether bacterial antigen/cell contact was sufficient to trigger E-cad modulation, or
303 whether infection was absolutely required to observe a change in E-cad expression. Thus, we
304 investigated by confocal microscopy E-cad expression on BeWo cells after 4 hours and 24 hours
305 of infection with live *C. burnetii,* while controls consisted of exposure to heat-inactivated bacteria
306 or LPS. Although for unstimulated BeWo cells a high level of fluorescence and homogeneity of E-
307 cad distribution was observed, this result was not limited to this experimental condition. The same

308 expression profiles were observed for BeWo cells after *E. coli* LPS stimulation or heat-inactivated
309 *C. burnetii* bacterium stimulation (**Figure 2D**). Interestingly, live *C. burnetii*-infected BeWo cells
310 presented a significant decrease of E-cad expression and also a short intracellular colocalization of
311 the E-cad fluorescence signal with the fluorescence signal associated with *C. burnetii* at early stage
312 of infection (**Figure S2**). In contrast, a low E-cad fluorescence signal was observed in infection
313 (live *C. burnetii*-infected BeWo cells). This decrease of E-cad cell-surface expression was
314 accompanied by an actin rearrangement over time (as shown at 24 hours) which was faster when
315 the cells where infected with the virulent Guiana strain (**Figure S3**). These results indicate that
316 membrane-bound E-cad expression is highly modulated during active *C. burnetii* infection of
317 BeWo cells, while *C. burnetii* bacterial antigens are not sufficient to trigger a massive E-cad
318 modulation.
319

320 **Release of sE-cad by *C. burnetii*-infected BeWo cells and modulation of *CDH1/*E-cad and**
321 ***CTNNB1*/β-catenin gene transcription**

322 Since we previously reported that Q fever patients have high expression of serum sE-cad[27], we
323 aimed at investigating whether the decreased expression of membrane-bound E-cad in *C. burnetii*-
324 infected BeWo cells could be associated with a release of sE-cad after E-cad proteolysis. As shown
325 in **Figure 3A**, we measured progressive basal accumulation of sE-cad in the cell culture medium
326 over time (at 24 hours and 48 hours). Interestingly, sE-cad release was significantly higher ($p$
327 $<0.001$) over time in infection conditions compared to control conditions (unstimulated and LPS-
328 stimulated BeWo cells). A further immunoblot detection of the products synthesized in *C. burnetii*-
329 infected cells evidenced two components: the integral 120 kDa E-cad, and a protein of about 60
330 kDa, a proteolytic product of E-cad (**Figure 3C**). In contrast, only the 120 kDa E-cad was found in
331 the control experiments. It is worth noting that the expression of β-catenin, an intracellular ligand

332 of E-cad, was strongly decreased in BeWo cells under live *C. burnetii*-infection conditions. This
333 was further confirmed using a densitometry scanning of the band that showed a significant ($p<0.05$)
334 decrease of β-catenin in *C. burnetii*-infected BeWo cells.
335 In accord with the literature regarding the E-cad/β-catenin signaling pathway, our results suggest
336 a translocation of β-catenin into the cell nucleus, associated with a modulation of *CDH1*/E-cad
337 gene expression. To confirm this hypothesis, the expression of *CDH1*/E-cad and *CTNNB1*/β-
338 catenin gene transcription was analyzed by qRT-PCR. Both *CDH1* and *CTNNB1* genes were found
339 significantly overexpressed ($p<0.01$ and $p<0.05$, respectively) in BeWo cells with *C. burnetii*
340 infection compared to cells exposed to *E. coli*-LPS (**Figure 3B**). These results indicate that *C.*
341 *burnetii* infection of BeWo cells induces a shedding of the E-cad protein ectodomain at an early
342 stage of the infection (detectable at 24 hours post-infection) and suggest that sE-cad shedding is
343 associated with the nuclear translocation of β-catenin and subsequent up-regulation of *CDH1* and
344 *CTNNB1* gene transcription through a feedback control loop.
345
346 ***C. burnetii* modulates expression of genes from both the E-cad/β-catenin pathway and the**
347 **Wnt/frizzled/β-catenin pathway in BeWo cells.**
348 To further demonstrate that the overexpression of *CDH1* and *CTNNB1* genes found in *C. burnetii*
349 infection of BeWo cells is not strain-dependent, BeWo cells were exposed for 48 hours to either
350 the live Nine Mile strain of *C. burnetii* or the more virulent Guiana (Cb175) laboratory strains of
351 *C. burnetii.* Heat-inactivated *C. burnetii* (Nine Mile strain) and *E. coli* LPS were used as controls.
352 As shown in **Figure 4A and 4B,** a significant overexpression of *CDH1* and *CTNNB1* genes was
353 found in BeWo cells infected with each of the two live strains of *C. burnetii*, extending our earlier
354 observations, illustrated in **Figure 3C**. In contrast, when BeWo cells were exposed to heat-
355 inactivated bacteria, *CTNNB1* gene expression was further increased and *CDH1* was significantly

356 decreased. These data suggest that the interaction of bacterial antigens with BeWo cells is sufficient
357 to trigger signals leading to *CTNNB1* gene transcription, while induction of *CDH1* requires
358 infection.
359 We then explored the expression of several other genes known to encode proteins linked to the E-
360 cad/β-catenin and Wnt/frizzled/β-catenin axis, including *WNT3A*, *WNT5A*, *WNT9b*, *FZD1*, *APC*,
361 *NKD2*, *BCL9*, *TCF7L2* and *CNND1*. As shown in **Figure 4C**, most of these genes were
362 overexpressed in *C. burnetii*-infected BeWo cells, some of which (e.g., *BCL9*, *Wnt3A*) being also
363 overexpressed when BeWo cells were exposed to heat-inactivated-bacteria infected cells. Notably,
364 *BCL9*, *WntA3*, and *FDZ1* genes were significantly overexpressed where cells were infected with
365 the live and more virulent Guiana strain of *C. burnetii* compared to infection with the live Nine
366 Mile strain. We also observed that the gene coding for the tumor suppressor *APC* was significantly
367 overexpressed after BeWo cell exposure to *E. coli* LPS. It is worth noting that the *CCND1* gene
368 coding for cyclin D1 kinase, a cell cycle activator and oncogenic protein, was significantly over-
369 transcribed in cells infected with live *C. burnetii*, notably in cells infected with the Nine Mile strain.
370 The *CCND1* gene is much less expressed with heat-inactivated bacteria, suggesting that activation
371 of this gene requires infection of cells by live bacteria. In addition, we also used a micro-array
372 technology to compare the expression of a set of 45000 genes in BeWo cells, infected or not by *C.*
373 *burnetii*. This approach indicated that 12189 genes were down-modulated after live *C. burnetii*
374 infection of BeWo cells, while 6492 genes were found up-regulated, among which genes such as
375 *CDH1, CCND1, and FZD1* were found highly expressed compared to their transcription levels in
376 uninfected BeWo cells (**Figure S4**).
377 The transcriptomic results illustrated in Figure 4 were subjected to a principal component analysis
378 (PCA) and a hierarchical clustering heatmap was regenerated. This analysis highlighted distinct
379 gene expression profiles (**Figure 5**), the first one corresponding to live *C. burnetii* strain infectious

380 conditions, with slight differences between live *C. burnetii* strains, while other profiles
381 corresponded to unstimulated cells, LPS stimulated cells and cells exposed to heat-inactivated *C.*
382 *burnetii*. Genes activated by the live *C. burnetii* strain infection cluster together and show a
383 mirrored gene expression compared to other conditions. These results indicate that live *C. burnetii*
384 specifically induce *CDH1*, *CCND1, CTNNB1* and *BCL9* gene overexpression in BeWo cells.
385 However, for induction of the BCL9 gene, infection is not required, and transcription can be
386 stimulated by simply exposing the cells to *C. burnetii* bacterial antigens.
387

388 **Discussion**

389 We report here the first experimental evidence that differential gene expression analysis shows
390 modulation of the E-cadherin/β-catenin pathway signature during *C. burnetii* infection *in vitro* and
391 that this modulation results in disruption of E-cad expression on the cell surface. As a strictly
392 intracellular bacterium, and in order to establish a replication niche, *C. burnetii* forms intimate
393 interactions with its hosts, which aid in avoidance of the host immune response. In addition to the
394 immune response, *C. burnetii* must overcome another central host defense mechanism, apoptosis.
395 The molecular crosstalk between the bacterium and the host affects the induction of apoptosis,
396 thereby prolonging its survival.
397 We previously reported that activation of protein tyrosine kinases (PTK) by *C. burnetii* in TPH-1
398 monocytes reflects *C. burnetii* virulence, since avirulent variants were unable to stimulate
399 PTK[55]. Additionally, modulation of cell signaling following *in vitro C. burnetii* infection of the
400 TPH-1 human macrophage-like cell line was also reported by Voth and Heinzen[56], who found
401 that infection directs the sustained activation of host pro-survival kinases Akt and Erk1/2, necessary
402 for anti-apoptotic activity that can conduct the development of certain lymphomas. Menelotte et
403 al.[22] were able to link the development of B-cell non-Hodgkin lymphoma to *C. burnetii* infection.

404 Despite intensive work to identify the bacterial compounds supporting *C. burnetii* replication and
405 virulence[11–13], the molecular mechanisms involved in *C. burnetii*-induced Q fever and possibly
406 associated NHL remain largely unknown. In more recent investigations[26] and working on Q
407 fever patient samples, we found that specific genes involved in anti-apoptotic processes (e.g., *BCL-*
408 *2*) were highly expressed, whereas pro-apoptotic genes were repressed in PBMCs from patients
409 with *C. burnetii*-associated NHL, supporting possible involvement of the corresponding proteins
410 in lymphomagenesis. However, these results remain controversial since other studies have not
411 confirmed the link between Q fever and NHL[28],[29].
412 The aim of the present study was to investigate *in vitro* the ability of *C. burnetii* to induce a
413 modulation of the E-cad/β-cat axis during infection. For this purpose, BeWo cells, which are
414 susceptible to *C. burnetii* infection, were used for their high expression of E-cad at the cell
415 membrane. As a result, we were able to demonstrate that the presence of *C. burnetii* in the cells
416 triggers overexpression of most of the genes of the signaling pathway, in particular *CDH1* genes
417 coding for the E-cad protein. Indeed, E-cad is known as a tumor suppressor trans-membrane protein
418 that inhibits β-cat activity by sequestrating it into the cell cytoplasm through interaction *via* the E-
419 cad cytoplasmic domain. In addition, cleavage of the E-cad protein by proteases (known as
420 sheddases) and excretion of a soluble fraction of E-cadherin (sE-cad) can contribute to cellular
421 transformation through the loss of cell-to-cell adhesion[57]. This is considered to be a triggering
422 event, promoting translocation of β-cat to the nucleus, where it forms complexes with BCL9 and
423 T-cell factor (TCF), leading to transactivation of cell cycle genes such as cyclin kinase *D1/CCND1*
424 and increased cell proliferation[58,59]. Moreover, the generation of sE-cad through sheddases and
425 the subsequent nuclear re-localization of β-cat may be a critical indicator for cancer development.
426 The induction of carcinogenic cascades via the E-cad/β-cat axis was reported in gastric
427 adenocarcinoma associated with *Helicobacter pylori* infection, in which the bacterium activates

428 calpain sheddase[60], or in myeloid-cell dependent distal colon tumorigenesis associated with
429 *Bacteroides fragilis* toxin, a known bacterial sheddase[61,62]. We recently reported[27] that E-cad
430 is cleaved in cells infected by *C. burnetii*. We demonstrated that, in addition to modulating *CDH1*
431 expression at the transcriptomic level, infection with *C. burnetii* leads to disruption of E-cad at the
432 cellular surface of BeWo cells. Under infection conditions, we observed a reduction of E-cad
433 expression at the cell surface that is likely due to cleavage of the extracellular fraction of the
434 protein, as its concentration in the supernatant is continuously increasing over time and the *CDH1*
435 gene is overexpressed. In BeWo cells infected with live *C. burnetii*, we observed a remodeling of
436 the actin filament, which triggers a morphological change. This particular effect was reported for
437 the first time in the study of Meconi et al.[63,55], in which they showed that virulent *C. burnetii*
438 stimulated morphological changes in human monocytes via the reorganization of the actin
439 cytoskeleton. As E-cad is linked to the actin cytoskeleton through β-cat and α-cat, a rearrangement
440 of the actin bundle can modify the adhesive function of E-cad and play an active role in the
441 migratory activity of carcinoma cells[64]. In the case of *C. burnetii* infection, the bacterium,
442 through the disruption of E-cad, may exploit the actin cytoskeleton to modulate its internalization
443 by host cells. An interesting observation that emerged from this study concerns the decreased
444 amount of β-cat protein in the cells, even though it is overexpressed at the transcriptomic level in
445 cells infected with the live bacterium. As β-cat is part of the canonical Wnt-Frizzled/ β-cat pathway,
446 we investigated most of the gene operating in the axis and as a result the expression of the genes
447 *WNT3A* (encoding the extracellular Wnt molecules that bind Frizzled/low-density lipoprotein-
448 receptor related proteins (LPR) complex and act on the canonical Wnt signaling pathway),
449 *FZD1*/Frizzled (Wnt receptor), *NKD2* (Wnt pathway regulator protein) were significantly
450 overexpressed in cells infected with live bacterium, mainly those infected with the more virulent
451 Guiana strain (Cb175). Interestingly, it has been shown that the activation of the Wnt/ Frizzled//β-

452 catenin pathway led to altered expression of genes involved in cell cycle regulation and apoptosis
453 in normal and leukemic B-cell progenitors[65]. In a previous publication, an overexpression of
454 transcription factor TCF7L2 and BCL9 was found, which is known to promote tumor progression
455 by conferring enhanced proliferation, metastatic, and angiogenic properties to cancer cells[66].
456 This may indicate that in the extremely rare cases of patients with *C. burnetii*-associated NHL, a
457 possible activation signal leads to lymphoma initiation. Furthermore, we also note that the
458 expression of the tumor suppressor adenomatous polyposis coli (APC) is repressed in infected cells
459 compared to the other conditions, suggesting that *C. burnetii* promotes the canonical Wnt signaling
460 pathway. Similar results were obtained from the microarray analysis of the Wnt/Frizzled/β-catenin
461 pathways in BeWo cells gene expression. Obviously, we are well aware of having used in this
462 study a particular cell model, a human trophoblastic cell line, and that under these conditions there
463 is a risk to overstate the biological significance of our data with the aim of explaining certain
464 aspects of the pathophysiology of Q fever. In fact, B cell analysis, which would have been more
465 physiologically relevant, was not possible because the CD20+E-Cad+ cells represent less than 1%
466 of circulating B cells, as we published in a previous article[27]. However, this BeWo model is very
467 useful for studying the link between infection by *C. burnetii* and modulation of the expression of
468 E-cad and provided a possible molecular basis for explaining the increase in sE-cad concentrations
469 in sera of Q fever patients [27].
470 In conclusion, this work provides for the first time evidence of the disruption of E-cad both at the
471 transcriptomic and cell surface levels by *C. burnetii*, opening a new avenue of research in
472 understanding the pathophysiology of Q fever. We hypothesize that the cleavage of E-cad by *C.*
473 *burnetii* could be a means to ensure its transmigration in order to modulate the reactivity of immune
474 cells and thus facilitate *C. burnetii* progression towards the target organs. Upon further
475 investigation, we found that the cleavage of E-cad was mediated by a functional HtrA sheddase

476 encoded in the *C. burnetii* genome[67]. Hence, the release of sE-cadherin together with the
477 overexpression of Wnt/Frizzled/β-catenin may participate in the molecular crosstalk that occurs in
478 the lymph node microenvironment during persistent Q fever and, in very rare cases, triggering a
479 pro-carcinogenic program. Finally, it can be hypothesized that the decrease in the surface
480 expression of E-cad induced by *C. burnetii* influences the replication of the bacterium or its
481 virulence.
482

483 **Acknowledgments**

484 We thank Prof. Jean Christophe LAGIER and Didier RAOULT for stimulating discussions and
485 unwavering support.
486

487 **Funding**

488 This research received no external funding.
489
490
491
492
493
494
495
496
497
498
499

500 **References**

501 1. Maurin M, Raoult D. Q fever. Clin Microbiol Rev. 1999;12:518-53.

502 2. Baca OG, Li Y-P, Kumar H. Survival of the Q fever agent Coxiella burnetii in the
503 phagolysosome. Trends in Microbiology. 1994;2:476-80.

504 3. Ghigo E, Pretat L, Desnues B, Capo C, Raoult D, Mege J-L. Intracellular Life of Coxiella
505 burnetii in Macrophages: An Update. Annals of the New York Academy of Sciences.
506 2009;1166:55-66.

507 4. Ben Amara A, Ghigo E, Le Priol Y, Lépolard C, Salcedo SP, Lemichez E, et al. Coxiella burnetii,
508 the Agent of Q Fever, Replicates within Trophoblasts and Induces a Unique Transcriptional
509 Response. PLoS One. 2010;5:e15315.

510 5. Bechah Y, Verneau J, Ben Amara A, Barry AO, Lépolard C, Achard V, et al. Persistence of
511 Coxiella burnetii, the Agent of Q Fever, in Murine Adipose Tissue. PLoS One. 2014;9:e97503.

512 6. Raoult D, Marrie T, Mege J. Natural history and pathophysiology of Q fever. The Lancet
513 Infectious Diseases. 2005;5:219-26.

514 7. van Schaik EJ, Chen C, Mertens K, Weber MM, Samuel JE. Molecular pathogenesis of the
515 obligate intracellular bacterium Coxiella burnetii. Nat Rev Microbiol. 2013;11:561-73.

516 8. Melenotte C, Protopopescu C, Million M, Edouard S, Carrieri MP, Eldin C, et al. Clinical
517 Features and Complications of Coxiella burnetii Infections From the French National Reference
518 Center for Q Fever. JAMA Netw Open. 2018;1:e181580.

519 9. Thuny F, Grisoli D, Cautela J, Riberi A, Raoult D, Habib G. Infective Endocarditis: Prevention,
520 Diagnosis, and Management. Canadian Journal of Cardiology. 2014;30:1046-57.

521 10. Martinez E, Cantet F, Fava L, Norville I, Bonazzi M. Identification of OmpA, a Coxiella
522 burnetii protein involved in host cell invasion, by multi-phenotypic high-content screening. PLoS
523 Pathog. 2014;10:e1004013.

524 11. Martinez E, Allombert J, Cantet F, Lakhani A, Yandrapalli N, Neyret A, et al. Coxiella burnetii
525 effector CvpB modulates phosphoinositide metabolism for optimal vacuole development. Proc
526 Natl Acad Sci U S A. 2016;113:E3260-3269.
527 12. Shipman M, Lubick K, Fouchard D, Gurram R, Grieco P, Jutila M, et al. Proteomic and Systems
528 Biology Analysis of the Monocyte Response to Coxiella burnetii Infection. Wang T, éditeur. PLoS
529 ONE. 2013;8:e69558.
530 13. Stead CM, Omsland A, Beare PA, Sandoz KM, Heinzen RA. Sec-mediated secretion by
531 Coxiella burnetii. BMC Microbiol. 2013;13:222.
532 14. Vodkin MH, Williams JC, Stephenson EH. Genetic Heterogeneity among Isolates of Coxiella
533 burnetii. Microbiology. 1986;132:455-63.
534 15. Hendrix LR, Samuel JE, Mallavia LP. Differentiation of Coxiella burnetii isolates by analysis
535 of restriction-endonuclease-digested DNA separated by SDS-PAGE. Microbiology.
536 1991;137:269-76.
537 16. Jäger C, Willems H, Thiele D, Baljer G. Molecular characterization of *Coxiella burnetii*
538 isolates. Epidemiol Infect. 1998;120:157-64.
539 17. Beare PA, Samuel JE, Howe D, Virtaneva K, Porcella SF, Heinzen RA. Genetic Diversity of
540 the Q Fever Agent, *Coxiella burnetii* , Assessed by Microarray-Based Whole-Genome
541 Comparisons. J Bacteriol. 2006;188:2309-24.
542 18. Hornstra HM, Priestley RA, Georgia SM, Kachur S, Birdsell DN, Hilsabeck R, et al. Rapid
543 Typing of Coxiella burnetii. Li W, éditeur. PLoS ONE. 2011;6:e26201.
544 19. Hoover TA, Culp DW, Vodkin MH, Williams JC, Thompson HA. Chromosomal DNA
545 Deletions Explain Phenotypic Characteristics of Two Antigenic Variants, Phase II and RSA 514
546 (Crazy), of the *Coxiella burnetii* Nine Mile Strain. Infect Immun. 2002;70:6726-33.
547 20. Toman R, Škultéty L. Structural study on a lipopolysaccharide from Coxiella burnetii strain

548 Nine Mile in avirulent phase II. Carbohydrate Research. 1996;283:175-85.
549 21. Q FEVER: REPORT OF A CASE SIMULATING LYMPHOMA. Ann Intern Med.
550 1957;47:1030.
551 22. Melenotte C, Million M, Audoly G, Gorse A, Dutronc H, Roland G, et al. B-cell non-Hodgkin
552 lymphoma linked to Coxiella burnetii. Blood. 2016;127:113-21.
553 23. van Roeden SE, van Houwelingen F, Donkers CMJ, Hogewoning SJ, de Lange MMA, van
554 der Hoek W, et al. Exposure to Coxiella burnetii and risk of non-Hodgkin lymphoma: a
555 retrospective population-based analysis in the Netherlands. The Lancet Haematology.
556 2018;5:e211-9.
557 24. Rothman N, Skibola CF, Wang SS, Morgan G, Lan Q, Smith MT, et al. Genetic variation in
558 TNF and IL10 and risk of non-Hodgkin lymphoma: a report from the InterLymph Consortium. The
559 Lancet Oncology. 2006;7:27-38.
560 25. Ghigo E, Capo C, Raoult D, Mege J-L. Interleukin-10 Stimulates *Coxiella burnetii* Replication
561 in Human Monocytes through Tumor Necrosis Factor Down-Modulation: Role in Microbicidal
562 Defect of Q Fever. Tuomanen EI, éditeur. Infect Immun. 2001;69:2345-52.
563 26. Melenotte C, Mezouar S, Ben Amara A, Benatti S, Chiaroni J, Devaux C, et al. A transcriptional
564 signature associated with non-Hodgkin lymphoma in the blood of patients with Q fever. Dolcetti
565 R, éditeur. PLoS ONE. 2019;14:e0217542.
566 27. Mezouar S, Omar Osman I, Melenotte C, Slimani C, Chartier C, Raoult D, et al. High
567 Concentrations of Serum Soluble E-Cadherin in Patients With Q Fever. Front Cell Infect
568 Microbiol. 2019;9:219.
569 28. van Roeden SE, van Houwelingen F, Donkers CMJ, Hogewoning SJ, de Lange MMA, van
570 der Hoek W, et al. Exposure to Coxiella burnetii and risk of non-Hodgkin lymphoma: a
571 retrospective population-based analysis in the Netherlands. Lancet Haematol. 2018;5:e211-9.

572 29. Weehuizen JM, van Roeden SE, Hogewoning SJ, van der Hoek W, Bonten MJM, Hoepelman
573 AIM, et al. No increased risk of mature B-cell non-Hodgkin lymphoma after Q fever detected:
574 results from a 16-year ecological analysis of the Dutch population incorporating the 2007-2010 Q
575 fever outbreak. Int J Epidemiol. 2022;dyac053.
576 30. Dash S, Duraivelan K, Samanta D. Cadherin-mediated host–pathogen interactions. Cellular
577 Microbiology [Internet]. 2021 [cité 18 mars 2022];23. Disponible sur:
578 https://onlinelibrary.wiley.com/doi/10.1111/cmi.13316
579 31. Ashton-Key M, Cowley GP, Smith ME. Cadherins in reactive lymph nodes and lymphomas:
580 high expression in anaplastic large cell lymphomas. Histopathology. 1996;28:55-9.
581 32. McCrea PD, Maher MT, Gottardi CJ. Nuclear Signaling from Cadherin Adhesion Complexes.
582 Current Topics in Developmental Biology [Internet]. Elsevier; 2015 [cité 23 mars 2022]. p. 129-96.
583 Disponible sur: https://linkinghub.elsevier.com/retrieve/pii/S0070215314000192
584 33. Vleminckx K, Vakaet L, Mareel M, Fiers W, Van Roy F. Genetic manipulation of E-cadherin
585 expression by epithelial tumor cells reveals an invasion suppressor role. Cell. 1991;66:107-19.
586 34. Christofori G, Semb H. The role of the cell-adhesion molecule E-cadherin as a tumour-
587 suppressor gene. Trends in Biochemical Sciences. 1999;24:73-6.
588 35. Pe N. Tumor suppressor gene E-cadherin and its role in normal and malignant cells. Cancer
589 Cell International. 2003;7.
590 36. Wells A, Yates C, Shepard CR. E-cadherin as an indicator of mesenchymal to epithelial
591 reverting transitions during the metastatic seeding of disseminated carcinomas. Clin Exp
592 Metastasis. 2008;25:621-8.
593 37. Izaguirre MF, Galetto CD, Baró L, Casco VH. E-Cadherin Dysfunction and Cancer. Journal of
594 Biosciences and Medicines. Scientific Research Publishing; 2019;7:42-67.
595 38. Na T-Y, Schecterson L, Mendonsa AM, Gumbiner BM. The functional activity of E-cadherin

596 controls tumor cell metastasis at multiple steps. Proc Natl Acad Sci USA. 2020;117:5931-7.
597 39. Grabowska MM, Day ML. Soluble E-cadherin: More Than a Symptom of Disease. Front Biosci
598 (Landmark Ed). 2012;17:1948-64.
599 40. Devaux CA, Mezouar S, Mege J-L. The E-Cadherin Cleavage Associated to Pathogenic
600 Bacteria Infections Can Favor Bacterial Invasion and Transmigration, Dysregulation of the
601 Immune Response and Cancer Induction in Humans. Front Microbiol. 2019;10:2598.
602 41. Aghababaei M, Hogg K, Perdu S, Robinson WP, Beristain AG. ADAM12-directed ectodomain
603 shedding of E-cadherin potentiates trophoblast fusion. Cell Death Differ. 2015;22:1970-84.
604 42. Capo C, Lindberg FP, Meconi S, Zaffran Y, Tardei G, Brown EJ, et al. Subversion of monocyte
605 functions by coxiella burnetii: impairment of the cross-talk between alphavbeta3 integrin and CR3.
606 J Immunol. 1999;163:6078-85.
607 43. Ghigo E, Imbert G, Capo C, Raoult D, Mege J-L. Interleukin-4 Induces *Coxiella burnetii*
608 Replication in Human Monocytes but not in Macrophages. Annals of the New York Academy of
609 Sciences. 2003;990:450-9.
610 44. Heystek HC, Mudde GC, Ohler R, Kalthoff FS. Granulocyte-macrophage colony-stimulating
611 factor (GM-CSF) has opposing effects on the capacity of monocytes versus monocyte-derived
612 dendritic cells to stimulate the antigen-specific proliferation of a human T cell clone. Clin Exp
613 Immunol. 2000;120:440-7.
614 45. Saito H, Kato A, Matsumoto K, Okayama Y. Culture of human mast cells from peripheral
615 blood progenitors. Nat Protoc. 2006;1:2178-83.
616 46. Winer J, Jung CKS, Shackel I, Williams PM. Development and Validation of Real-Time
617 Quantitative Reverse Transcriptase–Polymerase Chain Reaction for Monitoring Gene Expression
618 in Cardiac Myocytesin Vitro. Analytical Biochemistry. 1999;270:41-9.
619 47. Shannon JG, Heinzen RA. Adaptive immunity to the obligate intracellular pathogen Coxiella

620 burnetii. Immunol Res. 2009;43:138-48.
621 48. Sireci G, Badami GD, Di Liberto D, Blanda V, Grippi F, Di Paola L, et al. Recent Advances
622 on the Innate Immune Response to Coxiella burnetii. Front Cell Infect Microbiol. 2021;11:754455.
623 49. Zarza SM, Mezouar S, Mege J-L. From Coxiella burnetii Infection to Pregnancy
624 Complications: Key Role of the Immune Response of Placental Cells. Pathogens. 2021;10:627.
625 50. Graham JG, Winchell CG, Kurten RC, Voth DE. Development of an *Ex Vivo* Tissue Platform
626 To Study the Human Lung Response to Coxiella burnetii. Roy CR, éditeur. Infect Immun.
627 2016;84:1438-45.
628 51. Dragan AL, Kurten RC, Voth DE. Characterization of Early Stages of Human Alveolar
629 Infection by the Q Fever Agent *Coxiella burnetii*. Roy CR, éditeur. Infect Immun. 2019;87:e00028-
630 19.
631 52. Coutifaris C, Kao LC, Sehdev HM, Chin U, Babalola GO, Blaschuk OW, et al. E-cadherin
632 expression during the differentiation of human trophoblasts. Development. 1991;113:767-77.
633 53. Lecuit M, Nelson DM, Smith SD, Khun H, Huerre M, Vacher-Lavenu M-C, et al. Targeting
634 and crossing of the human maternofetal barrier by *Listeria monocytogenes* : Role of internalin
635 interaction with trophoblast E-cadherin. Proc Natl Acad Sci USA. 2004;101:6152-7.
636 54. Coleman SA, Fischer ER, Howe D, Mead DJ, Heinzen RA. Temporal Analysis of *Coxiella*
637 *burnetii* Morphological Differentiation. J Bacteriol. 2004;186:7344-52.
638 55. Meconi S, Capo C, Remacle-Bonnet M, Pommier G, Raoult D, Mege J-L. Activation of Protein
639 Tyrosine Kinases by Coxiella burnetii: Role in Actin Cytoskeleton Reorganization and Bacterial
640 Phagocytosis. Infect Immun. 2001;69:2520-6.
641 56. Voth DE, Heinzen RA. Sustained Activation of Akt and Erk1/2 Is Required for *Coxiella*
642 *burnetii* Antiapoptotic Activity. Infect Immun. 2009;77:205-13.
643 57. Zheng G, Lyons JG, Tan TK, Wang Y, Hsu T-T, Min D, et al. Disruption of E-Cadherin by

644 Matrix Metalloproteinase Directly Mediates Epithelial-Mesenchymal Transition Downstream of
645 Transforming Growth Factor-β1 in Renal Tubular Epithelial Cells. The American Journal of
646 Pathology. 2009;175:580-91.
647 58. Marambaud P. A presenilin-1/gamma-secretase cleavage releases the E-cadherin intracellular
648 domain and regulates disassembly of adherens junctions. The EMBO Journal. 2002;21:1948-56.
649 59. Kourtidis A, Ngok SP, Anastasiadis PZ. p120 Catenin. Progress in Molecular Biology and
650 Translational Science [Internet]. Elsevier; 2013 [cité 23 mars 2022]. p. 409-32. Disponible sur:
651 https://linkinghub.elsevier.com/retrieve/pii/B9780123943118000182
652 60. O'Connor PM, Lapointe TK, Jackson S, Beck PL, Jones NL, Buret AG. Helicobacter pylori
653 Activates Calpain via Toll-Like Receptor 2 To Disrupt Adherens Junctions in Human Gastric
654 Epithelial Cells. Blanke SR, éditeur. Infect Immun. 2011;79:3887-94.
655 61. Wu S, Morin PJ, Maouyo D, Sears CL. Bacteroides fragilis enterotoxin induces c-Myc
656 expression and cellular proliferation. Gastroenterology. 2003;124:392-400.
657 62. Chung L, Thiele Orberg E, Geis AL, Chan JL, Fu K, DeStefano Shields CE, et al. Bacteroides
658 fragilis Toxin Coordinates a Pro-carcinogenic Inflammatory Cascade via Targeting of Colonic
659 Epithelial Cells. Cell Host & Microbe. 2018;23:203-214.e5.
660 63. Meconi S, Jacomo V, Boquet P, Raoult D, Mege J-L, Capo C. Coxiella burnetii Induces
661 Reorganization of the Actin Cytoskeleton in Human Monocytes. Infect Immun. 1998;66:5527-33.
662 64. Ayollo DV, Zhitnyak IY, Vasiliev JM, Gloushankova NA. Rearrangements of the Actin
663 Cytoskeleton and E-Cadherin–Based Adherens Junctions Caused by Neoplasic Transformation
664 Change Cell–Cell Interactions. Hartl D, éditeur. PLoS ONE. 2009;4:e8027.
665 65. Khan NI, Bradstock KF, Bendall LJ. Activation of Wnt/?-catenin pathway mediates growth
666 and survival in B-cell progenitor acute lymphoblastic leukaemia. Br J Haematol. 2007;138:338-48.
667 66. Mani M, Carrasco DE, Zhang Y, Takada K, Gatt ME, Dutta-Simmons J, et al. BCL9 Promotes

Tumor Progression by Conferring Enhanced Proliferative, Metastatic, and Angiogenic Properties to Cancer Cells. Cancer Res. 2009;69:7577-86.

67. Osman IO, Caputo A, Pinault L, Mege J-L, Levasseur A, Devaux CA. Identification and characterization of an HtrA sheddase produced by Coxiella burnetii [Internet]. bioRxiv; 2023 [cité 10 févr 2023]. p. 2023.01.26.525556. Disponible sur: https://www.biorxiv.org/content/10.1101/2023.01.26.525556v1

692 **Table 1. Specific primers used for q-RTPCR assays**

693

| Genes (symbols) | Primers sequence | |
|---|---|---|
| | Sense | Antisense |
| Adenomatous polyposis coli (*APC*) | AGC-ACT-CCA-CCA-CAT-CAT-TCA-C | TTA-GAA-CAC-ACA-CAG-CAG-GAC-A |
| β-catenin (*CTNNB1*) | TCC-CTT-GGC-TGA-GTA-TTT-CTT-C | CAC-TGC-CTC-TTT-CCT-TAC-ATC-C |
| B-cell CLL/lymphoma 9 protein (*BCL9*) | TGT-TTT-CTA-CCC-CAG-GAC-TCT-C | CTA-TCG-TCT-CTT-TCC-ACA-TCC-A |
| Cyclin-dependent kinase 1 (*CCND1*) | ATC-CAG-TGA-CAA-ACC-ATC-CAG-T | TTG-GGT-AGA-AAA-CCA-GCA-TCT-C |
| E-cadherin (*CDH1*) | GAA-GGT-GAC-AGA-GCC-TCT-GGA-T | GAT-CGG-TTA-CCG-TGA-TCA-AAA-T |
| Frizzled Class receptor 1 (*FZD1*) | CCC-TCC-TAC-CTC-AAC-TAC-CAC-TT | ATT-ACA-CAC-CAC-TCG-GTC-TTC-C |
| Naked cuticle 2 (NC2) | GCC-TTA-GAG-CCA-GGA-AAC-ATA-G | CGA-CAG-CAA-ACA-GCA-ACT-GAC |
| Transcription factor 7-like 2 (*TCF7L2*) | GCT-ACG-ACC-TTT-GCT-CTC-ATT-T | ATC-ACG-ACA-GGA-GGA-TTC-AGA-C |
| Wnt Family Member 3A (*WNT3A*) | TGA-GAC-GGGG-CTC-CTT-CGG-CA | TGG-AGC-CGG-GAT-TCT-TGCAGG-T |
| Wnt Family Member 5A (*WNT5A*) | CAG-CAT-TCC-ACA-AAC-ACT-T | TTC-ACC-ATT-CCA-CAG-AGA-GAG-A |
| Wnt Family Member 9B (*WNT9B*) | GGA-AAA-TAC-CAC-AAC-CCC-ACC-T | GAC-CAC-TGA-CCC-CTC-ATT-CTA-C |

694

695

696

697 **Figures and legends**

698 **Figure 1. Selection of a cellular *in vitro* model to study E-cad modulation.**

699 **(A)** Immunoblot detection of E-cad expression in protein lysates of various cell types including
700 HeLa, THP-1, MRC-5, and the BeWo cell line and primary human monocytes **(B)** Cellular
701 localization/distribution of E-cad protein (red), actin (green) and nucleus (blue) in three different
702 cell types (BeWo cells, MRC-5 cells, monocytes). Images were acquired using a confocal
703 microscope (Zeiss LSM 800) with a 63X/1.4 oil objective (Scale bar: 10 µm). (**C**) Scanning
704 electron microscopy images of the ultra-thin section of BeWo cells infected with virulent *Coxiella*
705 *burnetii* Nine Mile (**a**) or *Coxiella burnetii* Guiana strain (**c**). **(b)** and (**d**) respectively high
706 magnification of the boxed region in **(a)** and **(c)** show a vacuole-contained *Coxiella burnetii*-like
707 bacteria (white arrows).

A.

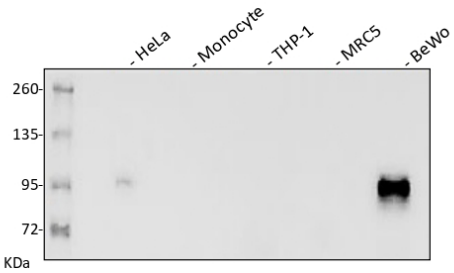


B.

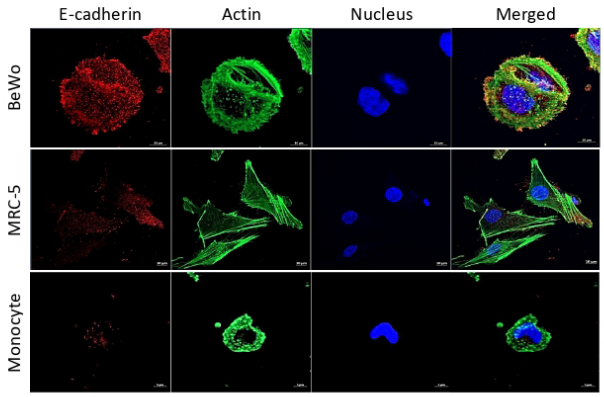


C.

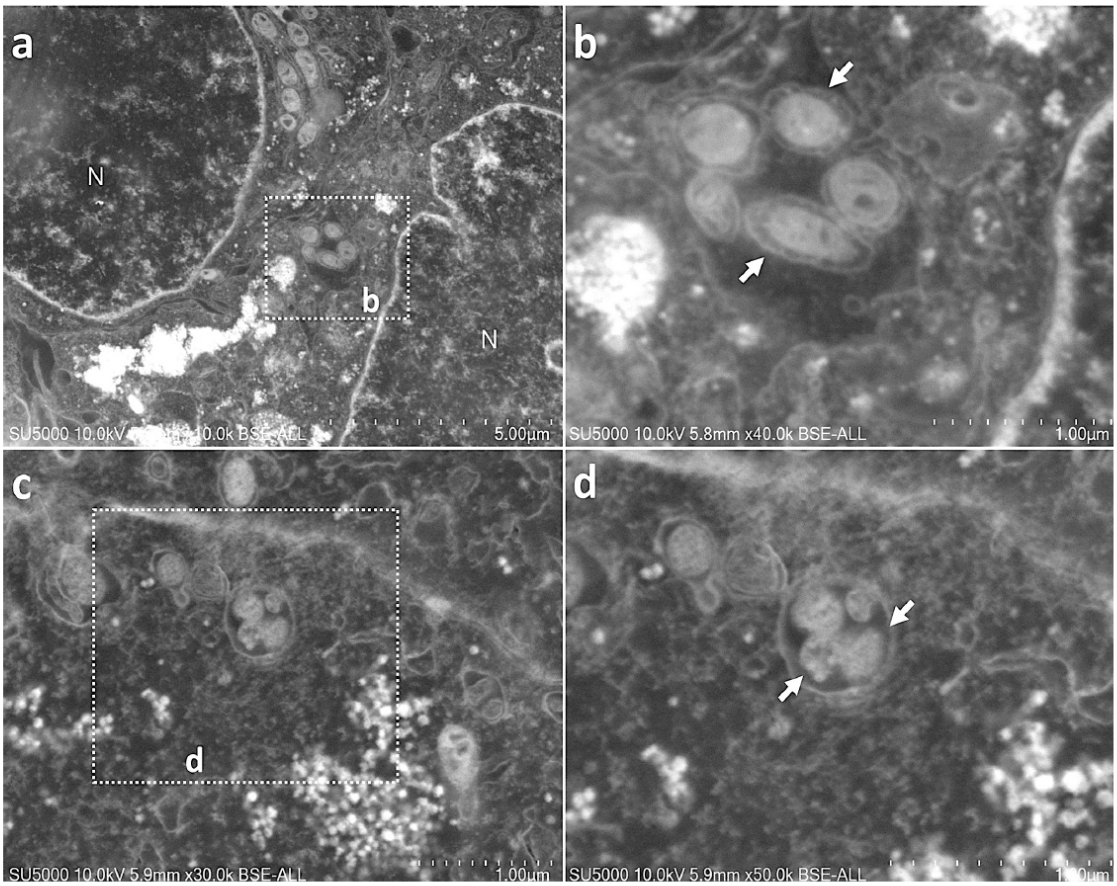


708

709

710

711 **Figure 2. Modulation of E-cad expression in BeWo cells either exposed to live *C. burnetii* or**
712 ***E. coli* LPS**.
713 (**A)** Flow cytometry analysis of E-cad expression at the surface of BeWo cells. Cells were incubated
714 with live *C. burnetii* Nine Mile strain or were stimulated with *E. coli* LPS for 24 hours (n = 3).
715 BeWo cells maintained in cultured medium without additive (unstimulated) were used as control.
716 The two panels show the gating parameter chosen and the quantification of E-cad, respectively.
717 **(B)** Histogram indicating the percent of cells expressing E-cad. **(C)** Histogram representing the
718 mean fluorescence intensity (MFI) under the different experimental conditions. The non-
719 parametric Mann-Whitney test was used for statistical analysis of all data. The p value < 0.05:
720 symbol *; p value <0.01: symbol **. **(D)** The panel presents *C. burnetii* (live or heat-inactivated
721 bacterium) exposed cells versus *E. coli* LPS stimulated cells and evaluation of fluorescence
722 corresponding to the E-cad (red), *C. burnetii* (white), actin (green), and the nucleus of the cells
723 (blue). Images were acquired using a confocal microscope (Zeiss LSM 800) with a 63X/1.4 oil
724 objective (scale bar: 20 µm).

A.

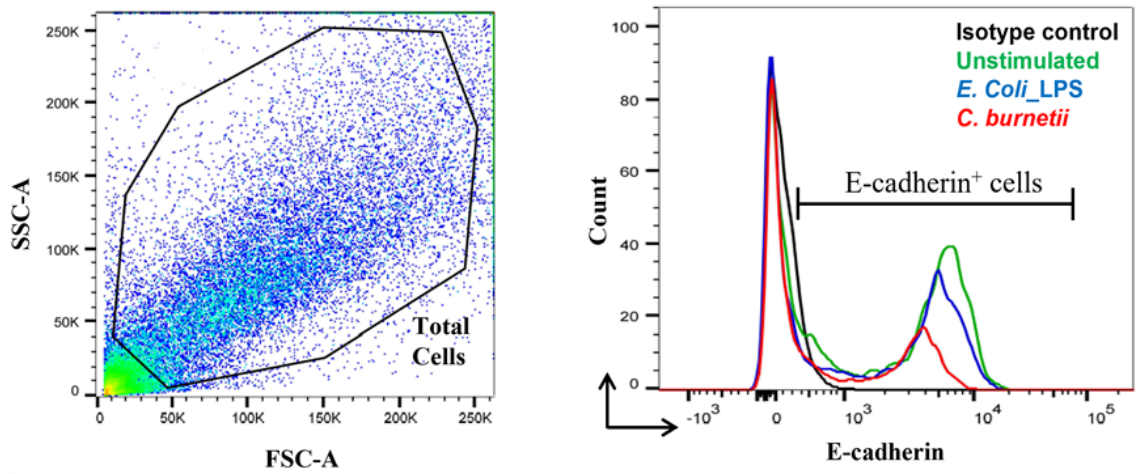
SSC-A
FSC-A
Total Cells
Isotype control
Unstimulated
E. Coli_LPS
C. burnetii
E-cadherin+ cells
Count
E-cadherin

B.

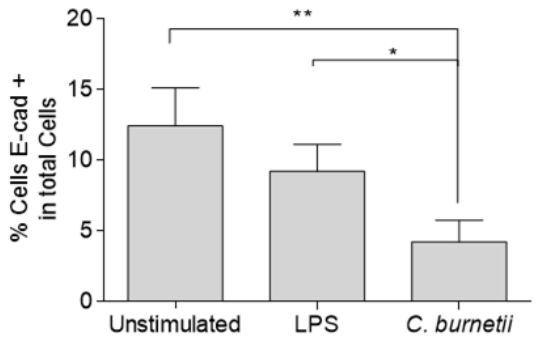
% Cells E-cad + in total Cells
Unstimulated
LPS
C. burnetii

C.

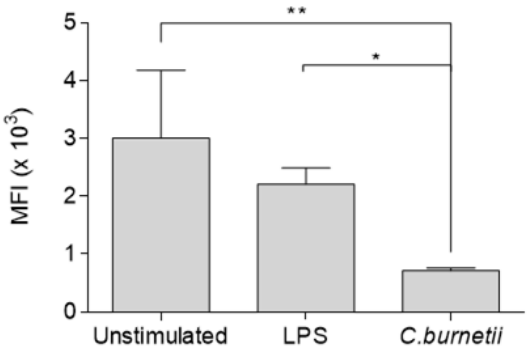
MFI (x 10^3)
Unstimulated
LPS
C.burnetii

D.

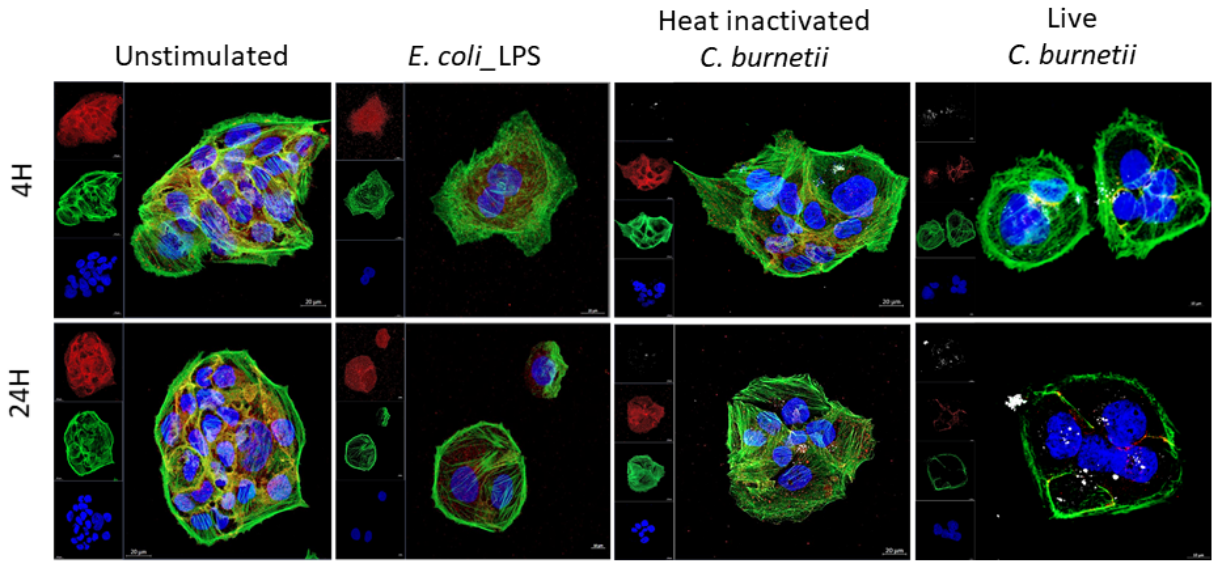
Unstimulated
E. coli_LPS
Heat inactivated C. burnetii
Live C. burnetii
4H
24H

725

726

727 **Figure 3. Impact of *C. burnetii* infection of BeWo cells on their E-cad expression**.

728 BeWo cells were incubated with live *Coxiella burnetii* Nine Mile strain for 4, 8, 24, and 48 hours
729 (n=3)**. (A)** ELISA quantification of sE-cad released in the supernatant of BeWo cells under
730 different experimental conditions (unstimulated, *E. coli* LPS-stimulated, *C. burnetii* Nine Mile
731 strain-infected), at different times of experiment. **(B)** qRT-PCR analysis of *CDH1*/E-cadherin and
732 *CTNNB1*/β-catenin mRNAs expression in BeWo cells exposed *in vitro* during 48 hours to *C.*
733 *burnetii* Nine Mile strain or the *E. coli* LPS. Expression level of investigated genes was illustrated
734 as ± SEM of the fold change ($FC = 2^{-\Delta\Delta Ct}$, where $\Delta\Delta Ct = [(Ct_{target} - Ct_{actin})$ stimulated$] - [(Ct_{target} -$
735 $Ct_{actin})$ unstimulated] and p values was evaluated according to an ordinary Two-way Anova test).
736 **(C)** Blots were spliced after protein transfer and then were probed with antibodies. Upper panel:
737 Immunoblot detection of E-cad (upper blot), β-catenin (middle blot) and β-actin (lower blot)
738 expression in total protein lysates of BeWo cells cultured under the three different experimental
739 conditions described above (unstimulated, LPS-stimulated, *C. burnetii*-infected), at 8 and 24 hours
740 post treatment. The histogram shown in the lower panel is a quantification of E-cad and β-catenin
741 expression (n=3) with respect to β-actin. The p value $< 0.05$: symbol *; p value $<0.01$: symbol **
742

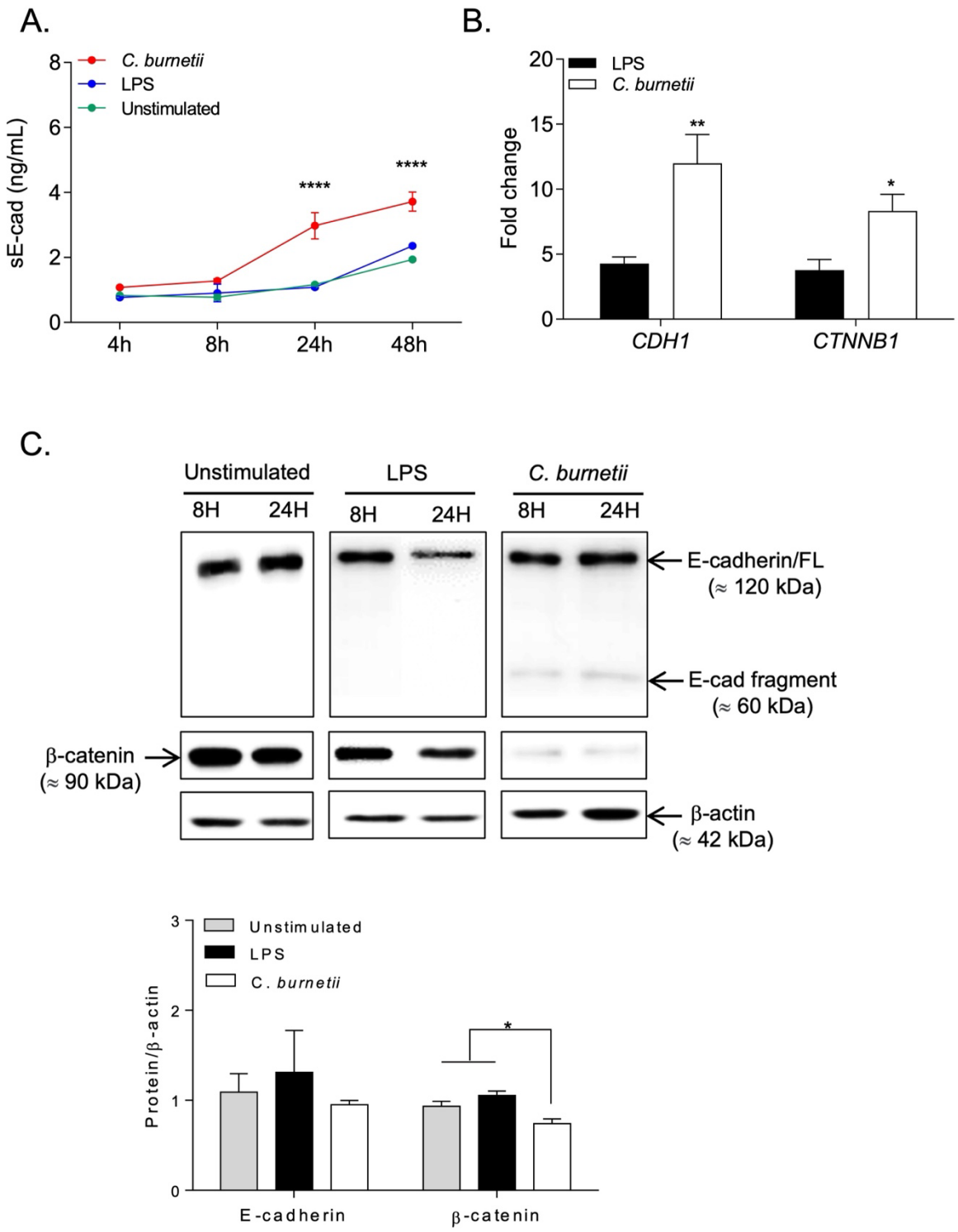
A.
C. burnetii
LPS
Unstimulated
sE-cad (ng/mL)
8
6
4
2
0
****
****
4h
8h
24h
48h
B.
LPS
C. burnetii
Fold change
20
15
10
5
0
**
*
CDH1
CTNNB1
C.
Unstimulated
LPS
C. burnetii
8H
24H
8H
24H
8H
24H
E-cadherin/FL
(≈ 120 kDa)
E-cad fragment
(≈ 60 kDa)
β-catenin
(≈ 90 kDa)
β-actin
(≈ 42 kDa)
Unstimulated
LPS
C. burnetii
Protein/β-actin
3
2
1
0
*
E-cadherin
β-catenin

743

744

745 **Figure 4**. **Impact of *C. burnetii* (Nine Mile strain or Guiana strain) infection of BeWo cells on**
746 **the expression of *CDH1*/E-cad, *CTNNB1*/β-catenin and other genes involved in the**
747 **Wnt/frizzled/β-catenin pathways.**

748 BeWo cells were exposed in *vitro* for 48 h to *C. burnetii* Nine Mile strain or Guiana (Cb 175) strain
749 (live and heat-inactivated strain) or were stimulated with *E. coli* LPS. The expression (n=6) of
750 *CDH1*/E-cad **(A)**, *CTNNB1*/β-catenin **(B)** and other genes involved in the Wnt/frizzled/β-catenin
751 pathways **(C to K)**, was investigated by qRT-PCR after normalization with the housekeeping actin
752 gene as endogenous control. Expression level of investigated genes was illustrated as ± SEM of
753 the fold change ($FC = 2^{-\Delta\Delta Ct}$, where $\Delta\Delta Ct = [(Ct_{target} - Ct_{actin})$ stimulated$] - [(Ct_{target} - Ct_{actin})$
754 unstimulated] and compared using the Kruskal-Wallis test. The p value < 0.05: symbol *; p value
755 <0.01: symbol **; p value < 0.001: symbol ***; p value <0.0001: symbol ****

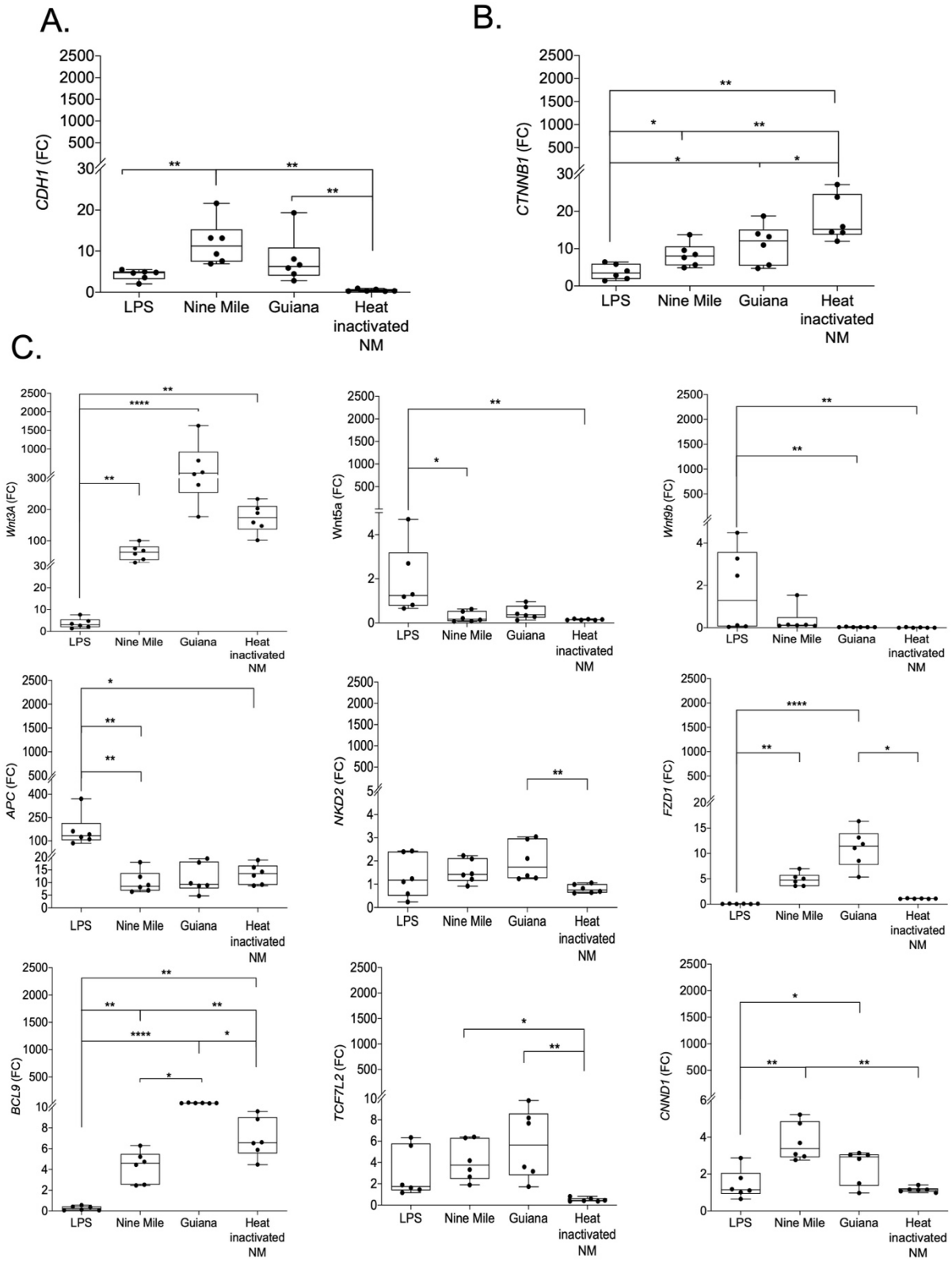
A.
CDH1 (FC)
LPS
Nine Mile
Guiana
Heat inactivated NM
B.
CTNNB1 (FC)
C.
Wnt3A (FC)
Wnt5a (FC)
Wnt9b (FC)
APC (FC)
NKD2 (FC)
FZD1 (FC)
BCL9 (FC)
TCF7L2 (FC)
CNND1 (FC)

756

757 **Figure 5. Principal component analysis and hierarchical clustering. BeWo cells were infected**
758 **or not with different strains of *C. burnetii* (live or heat inactivated) for 48 h**.
759 The transcripts of several genes were quantified by qRT-PCR. Results (n=6) were expressed as RE
760 $= 2^{-\Delta CT}$, where $\Delta ct = (Ct_{target} - Ct_{actin})$. Principal component analysis **(A)** and hierarchical clustering
761 **(B)** were performed to show the distribution of the different groups of infected/stimulated BeWo
762 cells and the modulation of expression of different genes, including *CDH1*/E-cad, *CTNNB1*/β-
763 catenin and other genes involved in the Wnt/frizzled/β-catenin pathways, such as WNT3A,
764 WNT5A, WNT9B.

A.

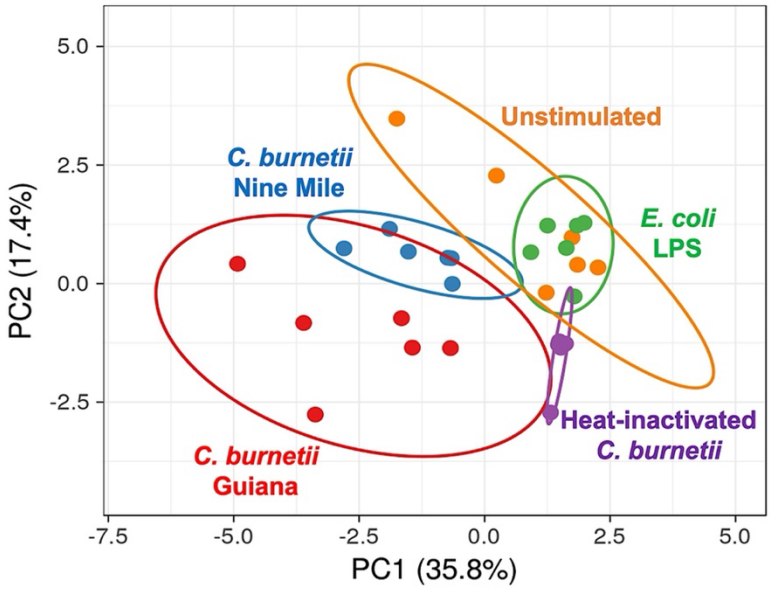
Unstimulated
C. burnetii
Nine Mile
E. coli
LPS
Heat-inactivated
C. burnetii
C. burnetii
Guiana
PC2 (17.4%)
PC1 (35.8%)
5.0
2.5
0.0
-2.5
-7.5
-5.0
-2.5
0.0
2.5
5.0

B.

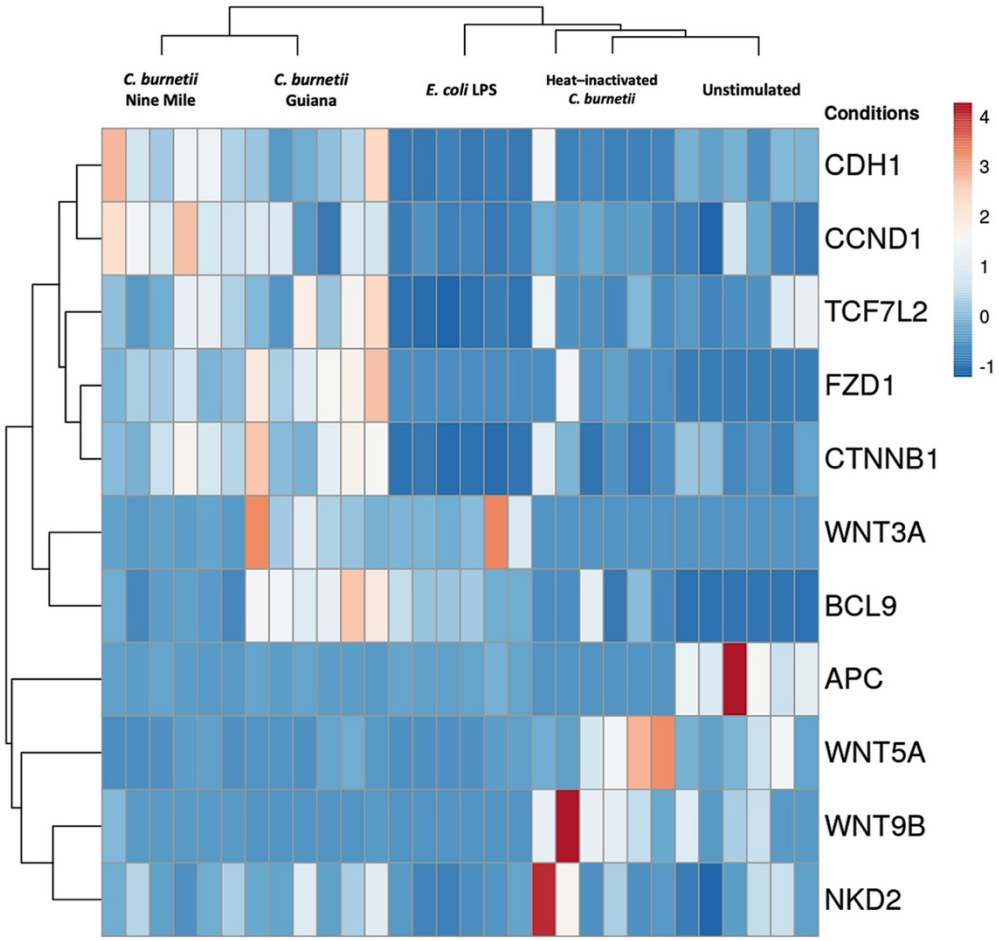
C. burnetii
Nine Mile
C. burnetii
Guiana
E. coli LPS
Heat–inactivated
C. burnetii
Unstimulated
Conditions
CDH1
CCND1
TCF7L2
FZD1
CTNNB1
WNT3A
BCL9
APC
WNT5A
WNT9B
NKD2
4
3
2
1
0
-1

765

766 **Supplementary data**

767 **Figure S1. Scanning electron microscopy images of the ultra-thin section of a trophoblast cell**
768 **incubated with *Coxiella* bacteria. (A, B, C)** SEM images of *C. burnetii* Guiana strain infected
769 BeWo cells. **(B)** High magnification of the boxed region in **(A)** shows serval vacuoles dispersed in
770 the cell cytoplasm. **(C)** High magnification of the boxed region in **(B)** shows a vacuole containing
771 electron-dense circular structures resembling *C. burnetii* (white arrows). **(D, E, F)** SEM images of
772 *C. burnetii* Nine Mile strain infected BeWo cells. **(D)** High magnification of the boxed region in
773 **(E)** shows vacuoles inside the BeWo cell **(F)** filled with hypo electron-dense *C. burnetii*-like
774 structures with or without less electron-dense internal content (white arrows).

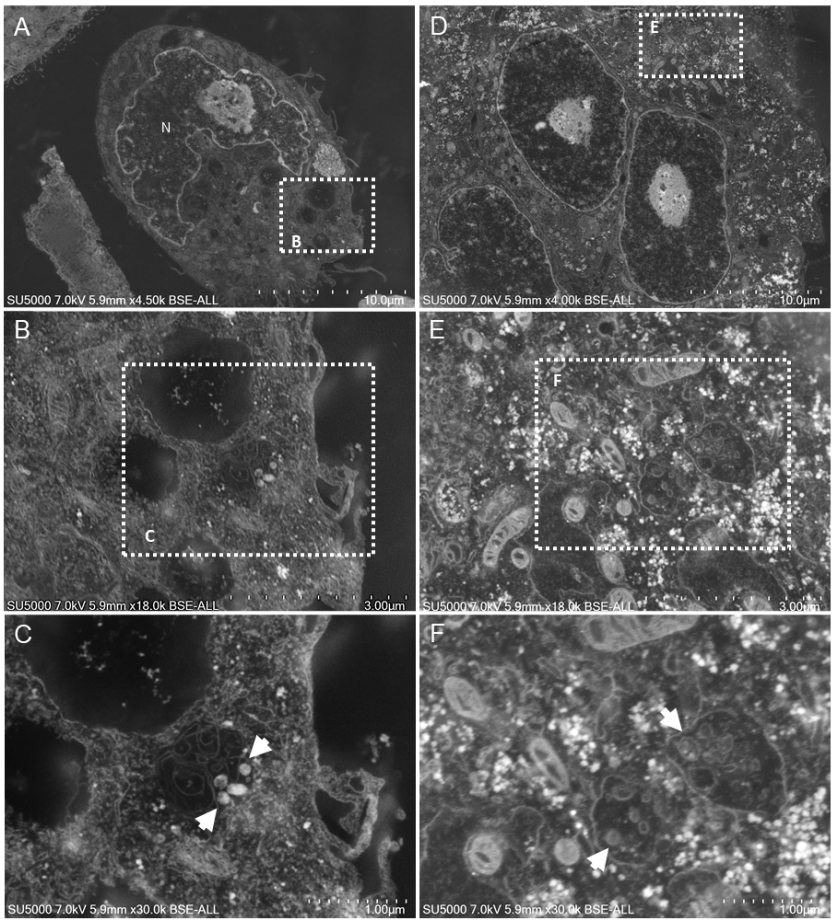


775

776 **Figure S2. Confocal microscopy analysis of BeWo cells at 5 min post-infection with *C.***
777 ***burnetii*.** Fluorescence labelling was as follows: *C. burnetii* (white), E-cad (red), actin (green), and
778 cell nucleus (blue). Images were acquired using a confocal microscope (Zeiss LSM 800) with a
779 63X/1.4 oil objective (scale bar: 10 µm). Regions of high concentration of *C. burnetii* are shown
780 with higher magnitude within scales.

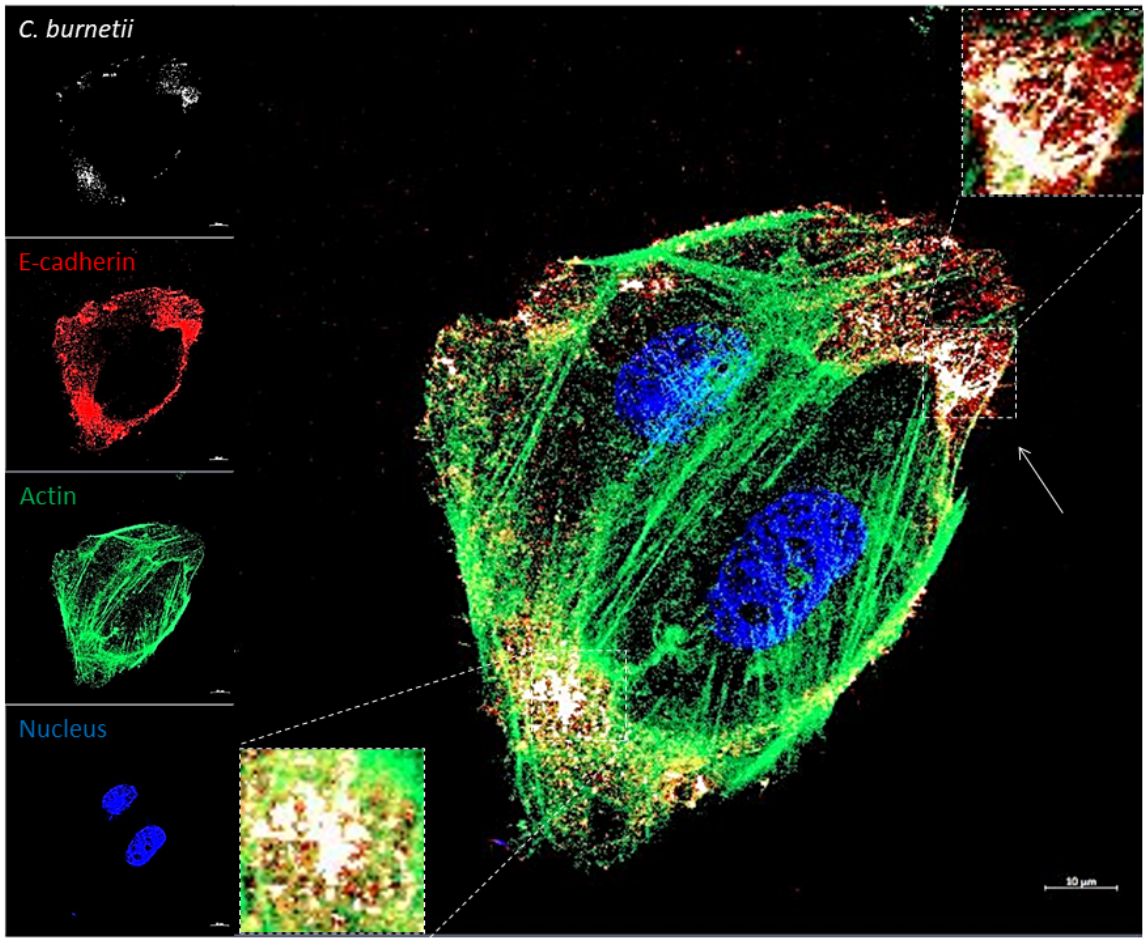


781
782
783
784
785
786

**Figure S3. Confocal microscopy analysis of BeWo cells at 4 hours post-infection with *C. burnetii* (Cb) Guiana strain.** Fluorescence labelling was as follows: *C. burnetii* (white), E-cad (red), actin (green), and cell nucleus (blue). Images were acquired using a confocal microscope (Zeiss LSM 800) with a 63X/1.4 oil objective (scale bar: 20 µm).

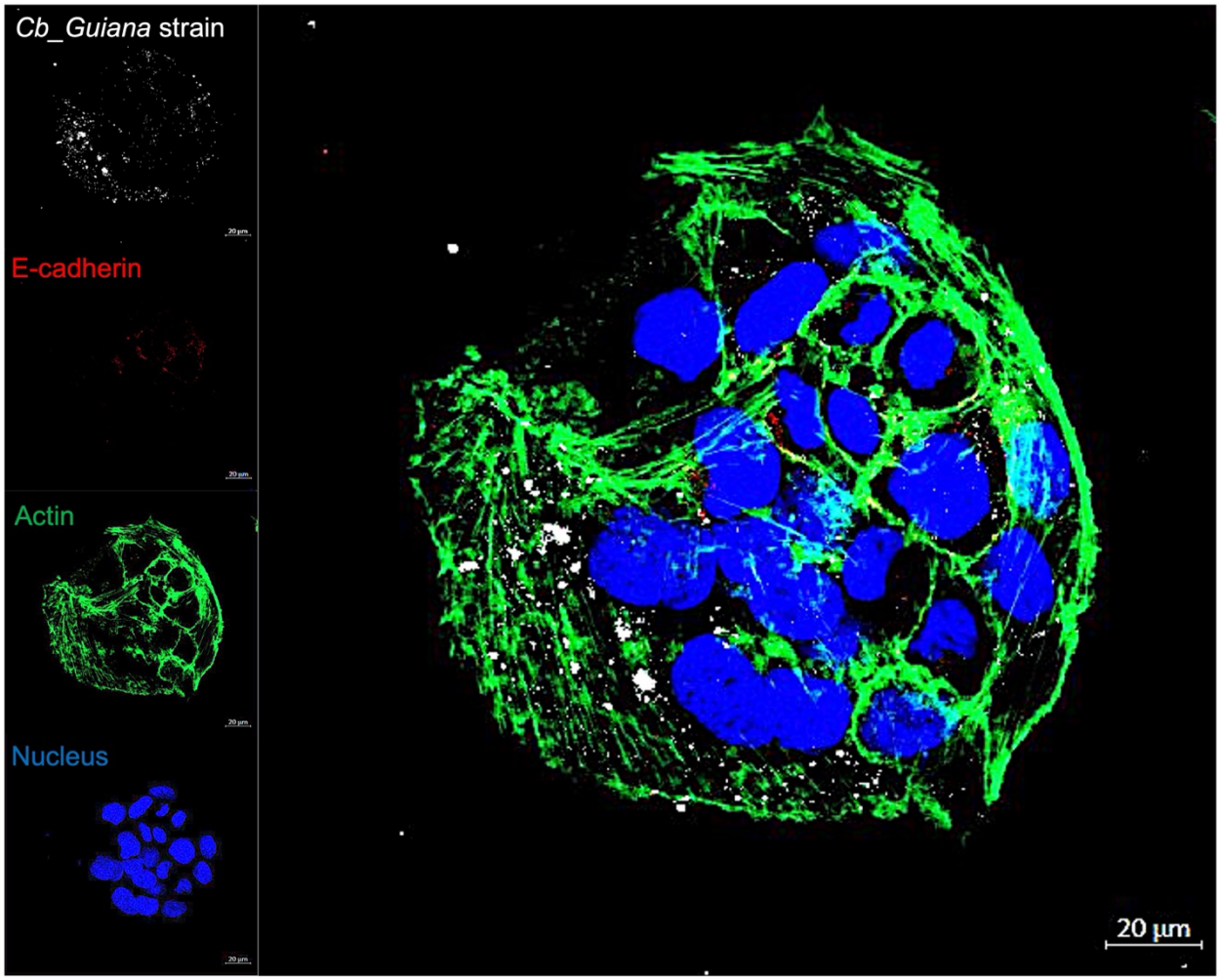

796 **Figure S4. Exploration of gene signatures of *C. burnetii* infection (Nine Mile laboratory**
797 **strain) of human cells as evidenced by microarray analysis.** BeWo cells infected or not by *C.*
798 *burnetii* were submitted to microarray analysis as well as primary cells, including monocyte-
799 derived macrophages (MDM), monocyte-derived dendritic cells (moDC), and mast cells. **(A)** Set
800 of genes up- or down-modulated in the panel of *C. burnetii* infected cells compared to uninfected
801 cells (e.g., 6942 genes up-regulated and 12199 genes down-regulated in BeWo cells after *C.*
802 *burnetii* infection). **(B)** principal component analysis and **(C)** hierarchical clustering were
803 performed to show the distribution of the different groups of infected cells and the modulation of
804 gene expression.
805
806

A.

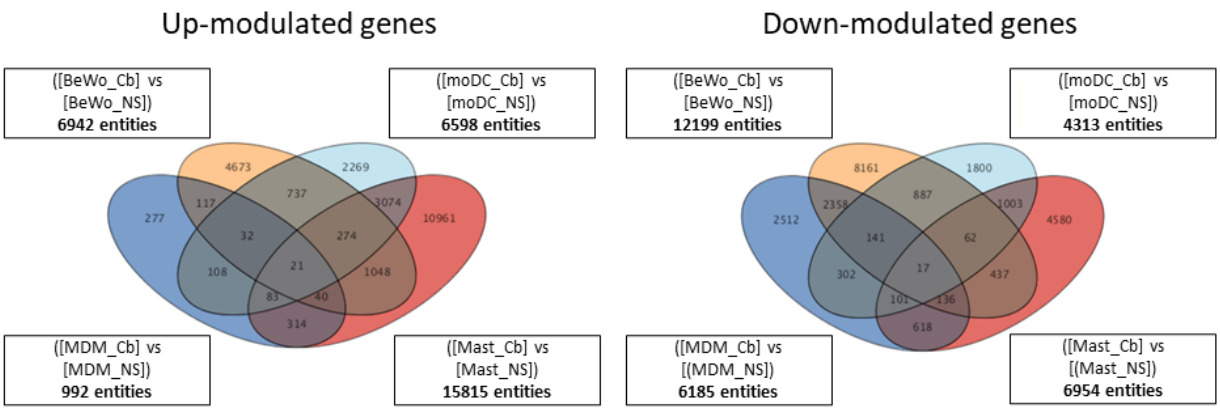
Up-modulated genes
([BeWo_Cb] vs [BeWo_NS]) 6942 entities
([moDC_Cb] vs [moDC_NS]) 6598 entities
([MDM_Cb] vs [MDM_NS]) 992 entities
([Mast_Cb] vs [Mast_NS]) 15815 entities
4673
2269
277
10961
117
737
3074
32
274
108
21
1048
83
40
314
Down-modulated genes
([BeWo_Cb] vs [BeWo_NS]) 12199 entities
([moDC_Cb] vs [moDC_NS]) 4313 entities
([MDM_Cb] vs [(MDM_NS]) 6185 entities
([Mast_Cb] vs [(Mast_NS]) 6954 entities
8161
1800
2512
4580
2358
887
1003
141
62
302
17
437
101
136
618

B.

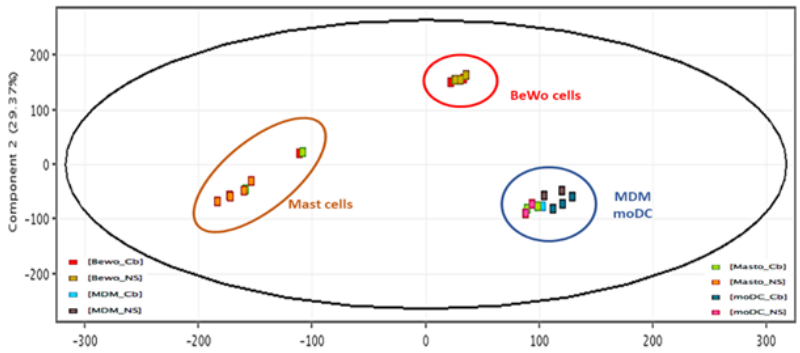
Component 2 (29.37%)
BeWo cells
Mast cells
MDM
moDC
[Bewo_Cb]
[Bewo_NS]
[MDM_Cb]
[MDM_NS]
[Masto_Cb]
[Masto_NS]
[moDC_Cb]
[moDC_NS]
200
100
0
-100
-200
-300
-200
-100
0
100
200
300

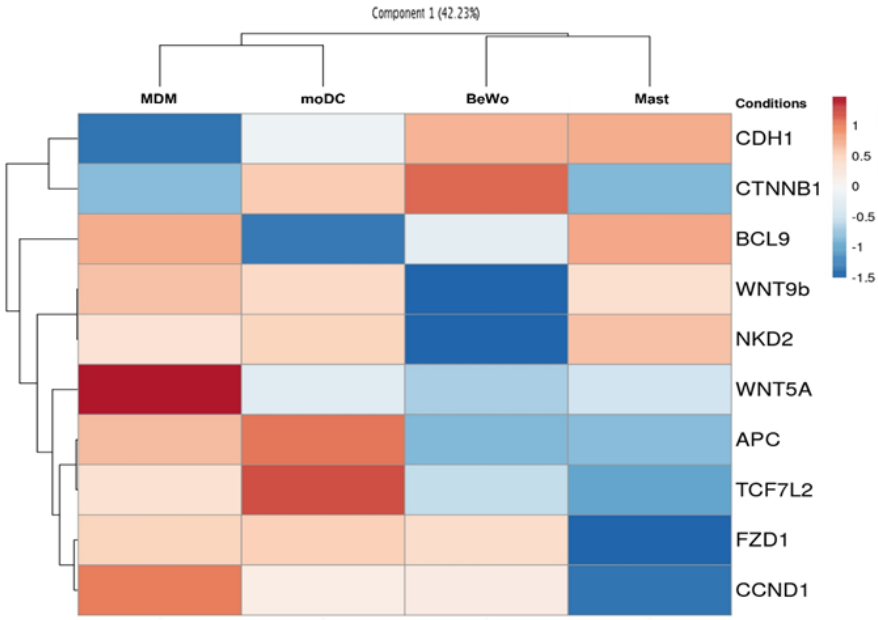
Component 1 (42.23%)
MDM
moDC
BeWo
Mast
Conditions
CDH1
CTNNB1
BCL9
WNT9b
NKD2
WNT5A
APC
TCF7L2
FZD1
CCND1
1
0.5
0
-0.5
-1
-1.5

807

808